JOURNAL OF GEOPHYSICAL RESEARCH, VOL. 91, NO. C9, PAGES 10,537–10,550, SEPTEMBER 15, 1986

Mapping Climatological Seasonal Variations of Surface Currents in the Tropical Atlantic Using Ship Drifts

PHILIP L. RICHARDSON AND DAVID WALSH

Woods Hole Oceanographic Institution, Woods Hole, Massachusetts

The seasonal variability of current velocities in the tropical Atlantic was studied by grouping ship drift velocity observations into 2° × 5° boxes and calculating monthly mean velocity values. These values were used to calculate and map the annual mean velocity, the seasonal variation about the mean, the annual and semiannual harmonics, and the first two empirical orthogonal functions (EOFs). The seasonal variation is primarily zonal in the equatorial band and in the North Equatorial Countercurrent (NECC) and primarily alongshore near the coast of South America. Maxima of seasonal variation of 23 cm/s are centered in the NECC near 6°N, 42.5°W and in the Gulf of Guinea near 2°N, 7.5°W. Most (~80%) of the variance in the NECC and along the western boundary of the area studied has an annual period; most of the variance along the equator in the mid-Atlantic has a semiannual period. Over the whole region, 49% of the seasonal variance is explained by the annual harmonic, and 69% is explained by a combination of the annual and semiannual harmonics. The second EOF contains 29% of the variance of the data set and shows a simultaneous speeding (slowing) of the major equatorial currents (the South Equatorial Current (SEC), the North Brazil Current, the NECC, and the Guinea Current) along their principal axes of variation with a concurrent slowing (speeding) of the Guyana Current and the Brazil Current. The pattern of variation resembles a large equatorial gyre centered along 4°N that flows clockwise from May to September and counterclockwise most of the rest of the year. The first EOF accounts for 35% of the variance and shows a simultaneous speeding (slowing) of eastward velocity from 5°S to 10°N except in the western SEC, the western end of the North Brazil Current, and the Guinea Current. The out-of-phase fluctuations apparent in the western SEC near the equator are explained by the slowing and reversal of the South Equatorial Current near 2°N, 40°W between April and June. This slowing of the SEC is associated with the start up of the NECC, which accelerates eastward in May, June, and July and flows eastward across the Atlantic from July through December. The SEC divides seasonally near the eastern tip of Brazil, where residual alongshore velocities are northward for half the year (peaking during May and June) and southward for the other half of the year. A second division can be seen north of the Amazon, where the North Brazil Current continues up the coast into the Guyana Current during the first half of the year but partially retroflects into the NECC during the last half of the year. A fast eastward flow in the NECC coincides with below average velocities in the Guyana Current and above average velocities in the western sections of the North Brazil Current and the SEC (north of the equator).

1. INTRODUCTION

Surprisingly little is known about the large-scale seasonal variability of the tropical Atlantic and how it is forced by wind stress and buoyancy flux. To remedy this, the Seasonal Equatorial Atlantic (SEQUAL) and Programme Français Océan Climat Atlantique Equatorial (FOCAL) field experiments were carried out between 1982 and 1984. The aim of these programs was to measure and model the response of the tropical Atlantic to seasonal wind forcing (SEQUAL, 1982; *Weisberg* [1984] and other papers in the same issue of *Geophysical Research Letters*). A major question that remains is how well measurements from relatively few sites, especially off the equator, represent long-term basin-wide seasonal variations. In an attempt to answer this question, historical ship drift data have been used to map the climatological variability of currents in the tropical Atlantic. Our objective is to describe basin-wide variability (1) to determine how and where the ocean is responding to seasonal forcing, (2) to provide a background for the analysis of the SEQUAL data, and (3) to map statistical characteristics of the variability, which will be helpful in making detailed comparisons between these data and numerical simulations of the tropical Atlantic circulation.

Paper number 6C0289.
0148-0227/86/006C-0289$05.00

The major cause of the large-scale velocity fluctuations in the equatorial region is the seasonally changing wind stress acting on the ocean surface (see reviews by *Philander* [1979], *Cane and Sarachik* [1983], and *Knox and Anderson* [1985]. Since energy can propagate rapidly along the equatorial wave guide and zonal geostrophic currents are easily generated there, variations in the wind forcing at one location can rapidly bring about changes in the near-surface flow in other areas. A key to understanding the ocean's large-scale response to wind forcing is to measure and correctly model the response of the surface layer, where the direct wind forcing occurs.

The only available direct measurements of surface current velocities made throughout the tropical Atlantic over a long time (~100 years) are historical ship drifts. Several papers and charts describing results from these data have been published [*Schumacher*, 1940, 1943; *Fuglister*, 1951; *Boisvert*, 1967; *Stidd*, 1975; *Wyrtki et al.*, 1976; *Duncan and Schladow*, 1981; *Meehl*, 1982; *U.S. Naval Oceanographic Office*, 1955, 1979]. A recent study [*Richardson and McKee*, 1984] used ship drifts to describe several features of the seasonal variation of the equatorial currents. Nevertheless, we thought that the data warranted a further, more statistical analysis. The present work extends the earlier Richardson and McKee study, using Fourier and empirical orthogonal function (EOF) techniques to map the characteristics of seasonal flow variations in the tropical Atlantic region. The major result is a clearer picture of where the main velocity

variations occur, how large they are, and how variations in one current are related to variations in other currents.

2. DATA

The ship drift data set was obtained from the U.S. Naval Oceanographic Office and consists of approximately 438,000 individual observations within the region bounded by 20°S–20°N, 10°E–70°W and the coasts of Africa and South America. Each ship drift measurement of surface current velocity consists of the vector difference between the actual velocity of a ship, determined from two position fixes, and the average estimated velocity of the ship through the water during the same time interval, usually 12–24 hours.

Observations were made throughout the whole tropical Atlantic, although they are clustered along the major shipping lanes. Our data cover the period from 1875 to 1976. However, a large percentage of the ship drift measurements were made between 1920 and 1940, so our results are strongly biased toward these years.

A nagging question about ship drifts is how good a measure they are of the real near-surface velocity. On the pessimistic side, each observation has a large random error, estimated to be ~20 cm/s from a consideration of errors in navigation and dead reckoning and from a comparison of drifting buoy and ship drift velocity [*Richardson*, 1983; *Richardson and McKee*, 1984]. A second, more serious problem is that systematic errors could exist because of the force of the wind and the waves on the ships. As we do not know the speed and direction steered by each ship nor the velocity of the wind blowing against it, we cannot investigate the possible effects of windage and wavage on the ship drift measurements. Even if we did know the concurrent wind, estimating its influence on a ship would be very tricky because a ship moves through two fluids, air and water, and the water is also responding to the wind. Accurately calculating the hydrodynamic lift on a ship due to the forces of wind and water acting on its hull would seem to be an almost impossible task. Furthermore, we have no knowledge of each ship's size, shape, loading, and methods of navigation or the competence of its navigators, nor of how these changed with time. Thus systematic errors remain unknown.

A more optimistic viewpoint is that the ship drift data set has some very useful properties. Each ship drift is an average over the ship's hull depth, over approximately half a day in time, and over a few hundred kilometers of the ship's trackline (commensurate with the size of a 2° × 5° box). Therefore each ship drift record tends to average over small scale fluctuations such as inertia gravity waves, current meanders, and eddies, leaving the larger-scale features which are of prime interest here. A second useful property is that numerous individual measurements exist from many years and from most regions of the tropical Atlantic. This enables us to group large numbers of drifts into each monthly value, significantly reducing the effects of random errors, of higher-frequency fluctuations such as the ~30-day instability waves observed near the boundary between the North Equatorial Countercurrent (NECC) and the South Equatorial Current (SEC), and of interannual variations.

A qualitative argument in favor of ship drifts is that maps of the mean velocity and seasonal variation make intuitive sense. Patterns look reasonable, values in adjacent boxes tend to agree in showing major features, and some smaller-scale features such as the double jets in the SEC are resolved. To assuage our doubts, we would like to have a detailed comparison of ship drifts with other direct current observations. However, since the ship drifts are largely from the period 1920–1940, they can only be compared with recent measurements in the climatic average sense. When this is done for regions of high velocity, the ship drifts tend to agree with other direct observations. A comparison of the average zonal velocity in the Gulf Stream determined by ship drifts, drifting buoys, and geostrophy showed that all three techniques agreed to a surprising degree in the amplitude and meridional shape of the velocity profile [*Richardson*, 1985]. A second comparison (in progress) of SEQUAL drogued drifting buoys and ship drifts in the NECC also shows some close agreement in the seasonal cycle. Of course, good agreement can only be expected when large numbers of observations are available and when drifting buoys are attached to drogues located in the mixed layer, which seems to act as a slab [*McNally*, 1981; *McNally and White*, 1985].

A very instructive recent study compares ship drifts, hydrographic data, winds, and model simulations throughout the tropical Atlantic [*Arnault*, 1984]. Arnault grouped ship drifts into 2° × 4° boxes and investigated the mean velocity and seasonal variation, much as has been done by *Richardson and McKee* [1984] and here. Her results agree with many of ours. But Arnault went a step further and compared the climatological ship drift velocities directly with (1) geostrophic velocities (referenced to 500 m) calculated from climatological density data and (2) Ekman velocities calculated from the climatological winds. Ship drift velocity was found to agree very closely with the sum of geostrophic velocity and Ekman velocity, both in the annual mean and in seasonal variations (outside of the narrow equatorial zone where $f \to 0$ and strong nonlinearities exist). The conclusion is that to the best of our knowledge, when ship drifts are suitably combined and averaged, they give a good measure of the seasonal variation of large-scale near-surface currents.

3. METHODS

Individual ship drift velocities were grouped into space-time bins, and average velocities were computed for each bin. To do this, we divided the tropical Atlantic region into 197 boxes, each covering 2° of latitude and 5° of longitude, in the area between 19°S and 19°N, 10°E and 70°W (Figure 1). To resolve seasonal variations, 12 monthly average values were computed for each box, with data from all available years grouped together. On the average, approximately 180 individual measurements were included in each monthly box average. Since the random error of an observation is approximately 20 cm/s [*Richardson*, 1983], the standard error of the mean for a monthly average velocity is approximately 1.5 cm/s, assuming that the individual measurements are statistically independent. Thus by using large numbers of observations to compute each average velocity value, the standard error has been reduced to well below the signal of the seasonal variation in most areas. Random errors should be smaller than this in the data-rich areas in the north and west, and larger in the data-poor regions in the south and east (Figure 1).

The monthly average velocities were used to compute the annual mean velocity components $\langle u \rangle$, $\langle v \rangle$ and the departures from this mean u', v', which we refer to as residual velocities. The magnitude of the seasonal variation is defined to be

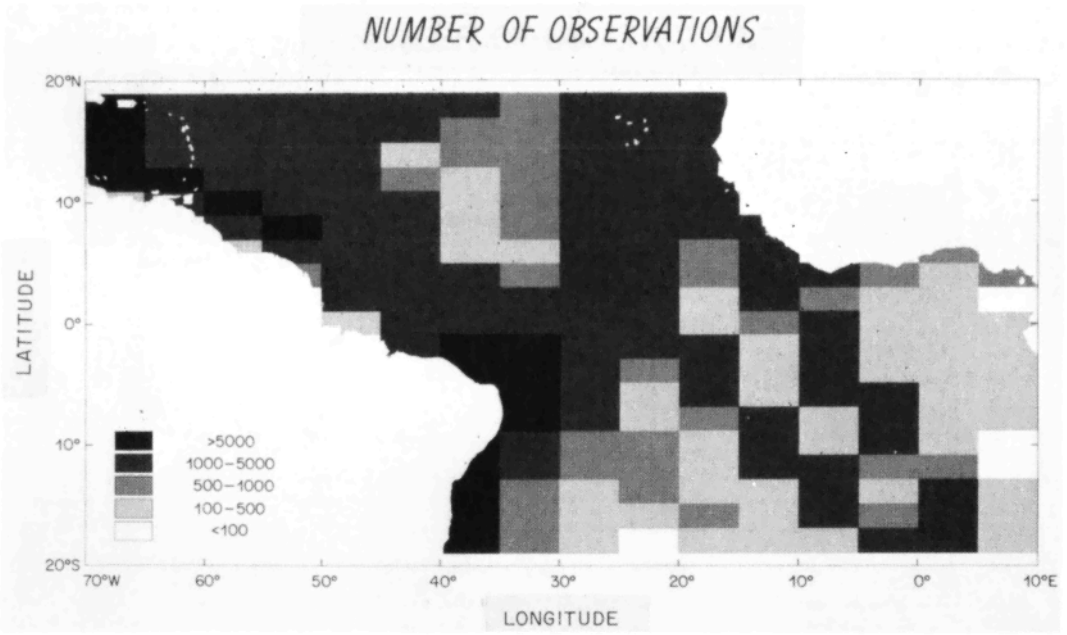

Fig. 1. Distribution in 2° × 5° boxes of the 438,000 individual ship drift velocity observations in the tropical Atlantic.

the standard deviation of velocity about the annual mean, calculated as follows: seasonal variation = $(\langle u'u' \rangle + \langle v'v' \rangle)^{1/2}$. Principal axes of seasonal variation were computed by rotating the axes in a direction such that the cross correlation of velocity components along the rotated axes vanished ($\langle u_r'v_r' \rangle = 0$). The length of an axis is proportional to the total velocity variance in the axis direction. The phases and amplitudes of the annual, semiannual, and higher-frequency harmonics were calculated using the u' and v' values. The total amplitude of a given harmonic A is given by $A = 1/2(A_x^2 + A_y^2)^{1/2}$ where A_x, A_y are the amplitudes for the zonal and meridional velocity components, respectively.

The residual velocities (u', v') were expanded in terms of empirical orthogonal functions to determine the principal modes of variability [see *Hardy and Walton*, 1978; *Kundu and Allan*, 1976; *Legler*, 1983]. The results are plotted as vector maps. At any given time, the length of the tail of each vector is proportional to the velocity associated with a given EOF mode. The time modulation of an EOF is determined by the associated coefficient time series, or principal components. The original velocity data at any time (minus the annual means) may be reconstructed by multiplying each EOF by the appropriate time series coefficient and summing over all modes. The principal components are complex valued, with the primary component being real and the secondary component imaginary. Each of the vectors in an EOF may be thought of as defining a rotated complex axis system, with the positive real axis in the direction of the vector and the positive imaginary axis oriented 90° counterclockwise from the real axis. Therefore the real part of the principal component time series denotes modulations along the axis of a vector, while the imaginary part denotes modulations at right angles to a vector, causing rotation. In our case the primary (real) component of the principal component time series contains virtually all of the variation, so the EOFs may be thought of as representing velocity modulations along the axes of the vectors, with essentially no rotation.

There is an angular ambiguity inherent in vector EOF analysis in that the principal component time series may be rotated through an arbitrary angle in the complex plane, provided that each vector in the associated EOF is rotated by an equal amount in the opposite direction. Therefore each of the EOFs was rotated through an angle chosen to give the clearest physical picture of the patterns of variation. To accomplish this, we required that (1) the primary and secondary components of the rotated principal component time series be mathematically uncorrelated and that (2) the majority of the variation be in the primary component. The fact that such a large proportion of the variation is confined to the primary component by this selection scheme is presumably a consequence of the fact that the major, large-scale velocity fluctuations in this region take place along well-defined axes.

4. Average Currents and the Seasonal Cycle

The general circulation of the tropical Atlantic is shown in a schematic map based on ship drift data from July to September (Figure 2) in maps which show mean velocity vectors and contours of the magnitude of the mean velocity (Figure 3) and in maps of the velocity in February, May, August, and November (Figure 4). Table 1 summarizes typical velocity values in specific currents. All surface currents are westward except the North Equatorial Countercurrent (seasonally) and the Guinea Current. The North Equatorial Current (NEC), located north of 10°N, is the southern part of the subtropical gyre, flowing westward as a broad current with a mean velocity of 10–15 cm/s. The South Equatorial Current consists of two parts: (1) a broad westward flow of 10–15 cm/s south of 10°S, the southern hemisphere equivalent of the NEC, and (2) a much swifter westward current along the equator, with a mean velocity of about 30 cm/s. This swifter part has two maxima in the west: a northern one with an annual average velocity of 33 cm/s at 2°N, 22.5°W, and a southern one with an average velocity of 37 cm/s at 4°S, 17.5°W. The southern part of the SEC impinges on the wedge-shaped eastern tip of Brazil and divides into a southward branch, the Brazil Current, with a mean velocity of 10–15 cm/s, and a northward branch, the

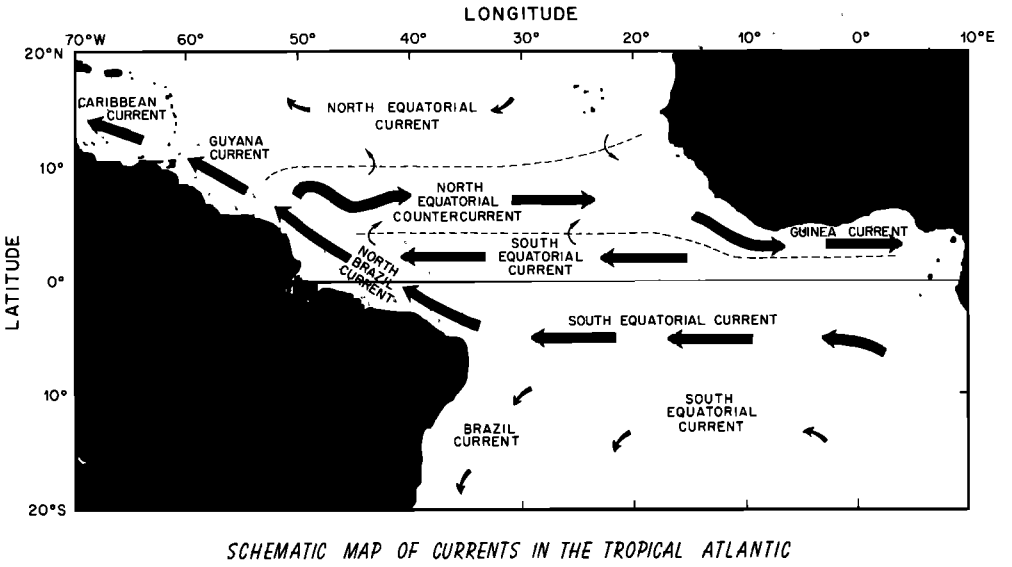

Fig. 2. Schematic map showing the major tropical currents between July and September, when the North Equatorial Countercurrent flows swiftly eastward across the Atlantic and into the Guinea Current. From January through June the countercurrent disappears, and westward velocities are seen in this area.

North Brazil Current, which crosses the equator and accelerates to a maximum velocity of 81 cm/s at 2°N, 47.5°W. In the western Atlantic, the northern part of the SEC near 2°N merges with the North Brazil Current and flows northwestward up the coast. During the last half of the year, the North Brazil Current divides near 8°N, 50°W. One part continues northwestward up the coast with velocities of 40–50 cm/s, first as the Guyana Current and then as the Caribbean Current. The other part turns offshore and flows eastward across the Atlantic as the North Equatorial Countercurrent (NECC), which has low annual mean velocities of 5–10 cm/s due to its seasonal reversal. This eastward flowing NECC flows into the Guinea Current, which flows eastward throughout the year, with a maximum mean velocity of 42 cm/s at 4°N, 7.5°W.

Many features of the seasonal cycle of velocity are seen in the monthly velocity maps (Figure 4). Major variations in velocity occur in three areas. The first is the western NECC, which flows eastward in a band centered between 5°N and 8°N from July through December. The maximum velocity is approximately 30 cm/s between July and September. West of 20°W and from January through June, the NECC disappears; westward velocities of 20 cm/s are observed in April and May near 40°W. The second area of large seasonal variation is near the boundary between the SEC and Guinea Current. This boundary shifts latitudinally during the year, causing the velocities at 2°N, 0°–10°W to change direction from east to west four times a year. During January, February, and August through October (approximately) the velocities are eastward; in November, December, and March through April velocities are westward. The third area is the northwestern SEC, where velocities decrease to near zero in April, May, and June near 3°N, 40°W, and actually reverse towards the east in May at 2°N, 37.5°W. This decrease and reversal of velocity is associated with the collapse of the easterly trade winds along the equator as the intertropical convergence zone (ITCZ) moves northward. When the winds relax, a zonal pressure gradient causes an eastward acceleration of the surface layer [*Katz et al.*, 1981]. Coinciding with this eastward acceleration is an increase in the speed (westward acceleration) of the North Brazil Current. Maps on a finer grid show that the patch of eastward flow propagates northwestward up the coast and becomes the NECC in July [see *Richardson and McKee*, 1984].

5. Seasonal Variation of Velocity

The seasonal variation of velocity about the annual mean is shown in three maps (Figure 5). The seasonal variation is small (3–4 cm/s) near 20°N and 20°S, and increases equatorward toward a band of high values (greater than 10 cm/s) between 5°S and 10°N. Within this band of high values are two equal maxima of about 23 cm/s. One is located in the Gulf of Guinea near the northern edge of the SEC, at 2°N, 7.5°W. Seasonal variations of greater than 15 cm/s surround this maximum, extending along the boundary between the Guinea Current and the SEC from 2°S to 4°N and from 5°E to 20°W. A band of high values extends westward across the Atlantic along 2°N in the northern part of the SEC. The second maximum is centered in the western NECC near 6°N, 42.5°W. Values of >15 cm/s extend southward to the North Brazil Current and eastward between 6°N and 8°N to 20°W. Between the two maxima, a minimum along 4°N from 18°–33°W coincides with the region of low mean velocities between the NECC and SEC.

The map of principal axes shows that most of the seasonal variation takes place in a zonal (east-west) direction in the NECC and SEC and is nearly parallel to the coast in the Caribbean, Guyana, North Brazil, Brazil, and Guinea Currents. For the most part, there does not appear to be a preferred direction outside of the band between about 6°S and 12°N.

The map of the ratio of seasonal to mean kinetic energy shows a large region of values of >1 from 3°–10°N, coinciding with the NECC. These high values reach a peak of 35 at 8°N, 27.5°W. (This is near the spot chosen to moor the SEQUAL NECC current meters, at 6°N, 28°W). The peak is due to a combination of a large seasonal variation (~15 cm/s) and a low mean velocity (~2 cm/s). A second peak ratio of 8

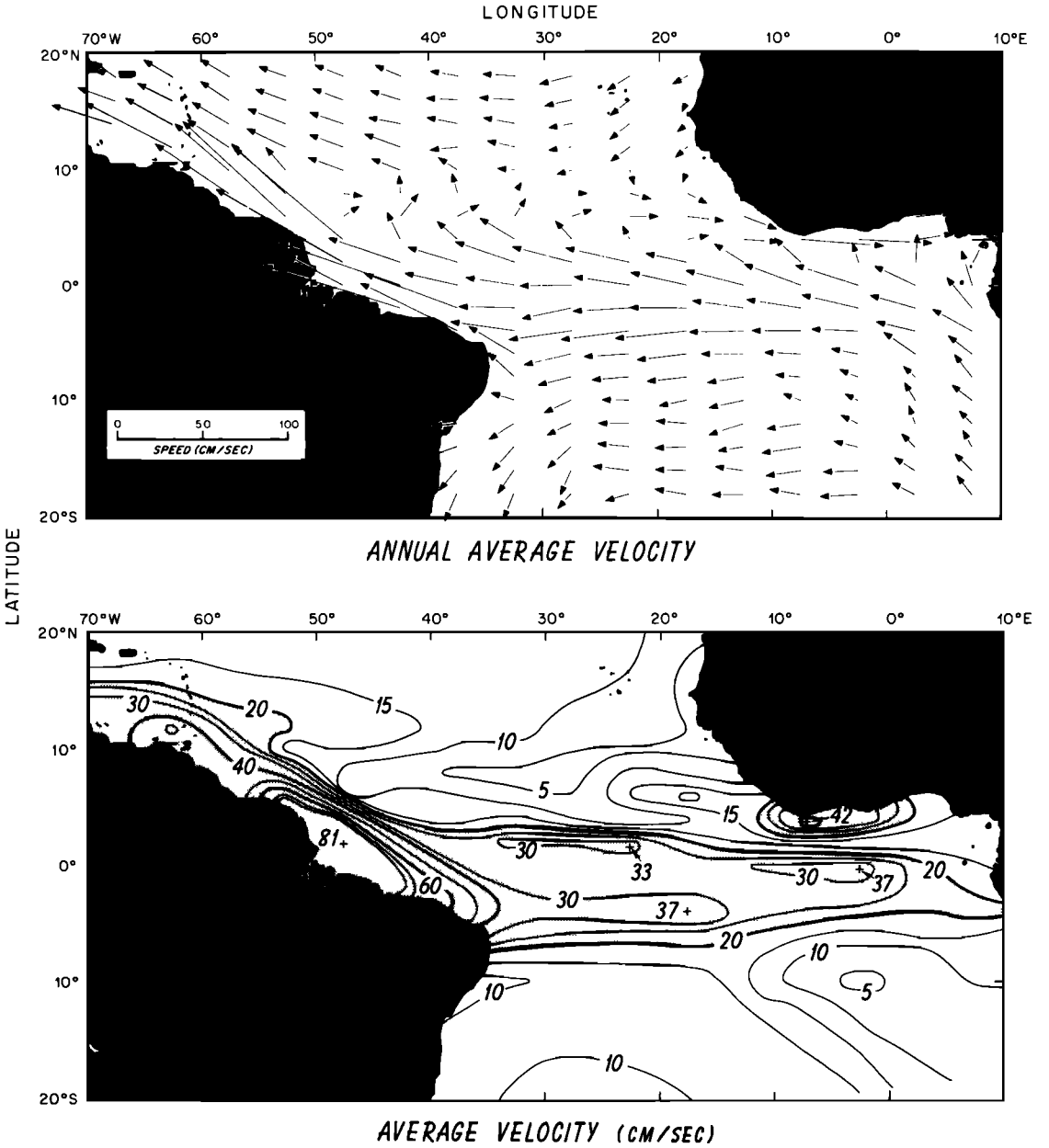

Fig. 3. (Top) Annual average velocity in each 2° × 5° box. Speed is proportional to the length of the tail of each vector. (Bottom) The magnitude of the annual average velocity. Velocities greater than 20 cm/s are shaded to emphasize the fastest currents.

exists near the crossover between the Guinea Current and SEC near 2°N, 2.5°W. This peak is again due to a large seasonal variation (~22 cm/s) and a low mean velocity (~8 cm/s).

6. Fourier Analysis

Results of the Fourier analysis are shown in three sets of maps. Figure 6 shows the amplitudes of the first two Fourier harmonics, with annual and semiannual periods, which account for most of the seasonal variation. Figure 7 shows the percentage of the seasonal variation accounted for by each harmonic. Figure 8 shows the amplitude and phase of the zonal component, which accounts for most of the seasonal variation outside the boundary currents. Table 1 is a summary of typical velocity values.

6.1. *Annual Harmonic*

The overall pattern of annual harmonic amplitudes (Figure 6) is similar to that of the magnitude of the seasonal variation (Figure 5). Values in the NECC/North Brazil Current and the peak of 23 cm/s are nearly the same as the seasonal variation values, clearly showing the predominance of annual period fluctuations in this area. In the Gulf of Guinea, however, the area of values of >15 cm/s and the peak value are significantly smaller for this harmonic than for the seasonal variation.

The map of the percentage of seasonal variance accounted for by the annual harmonic (Figure 7) shows that the highest values occur along the western boundary (80–90%), in the NECC (70–80%), and in the Guinea Current (60–70%). A

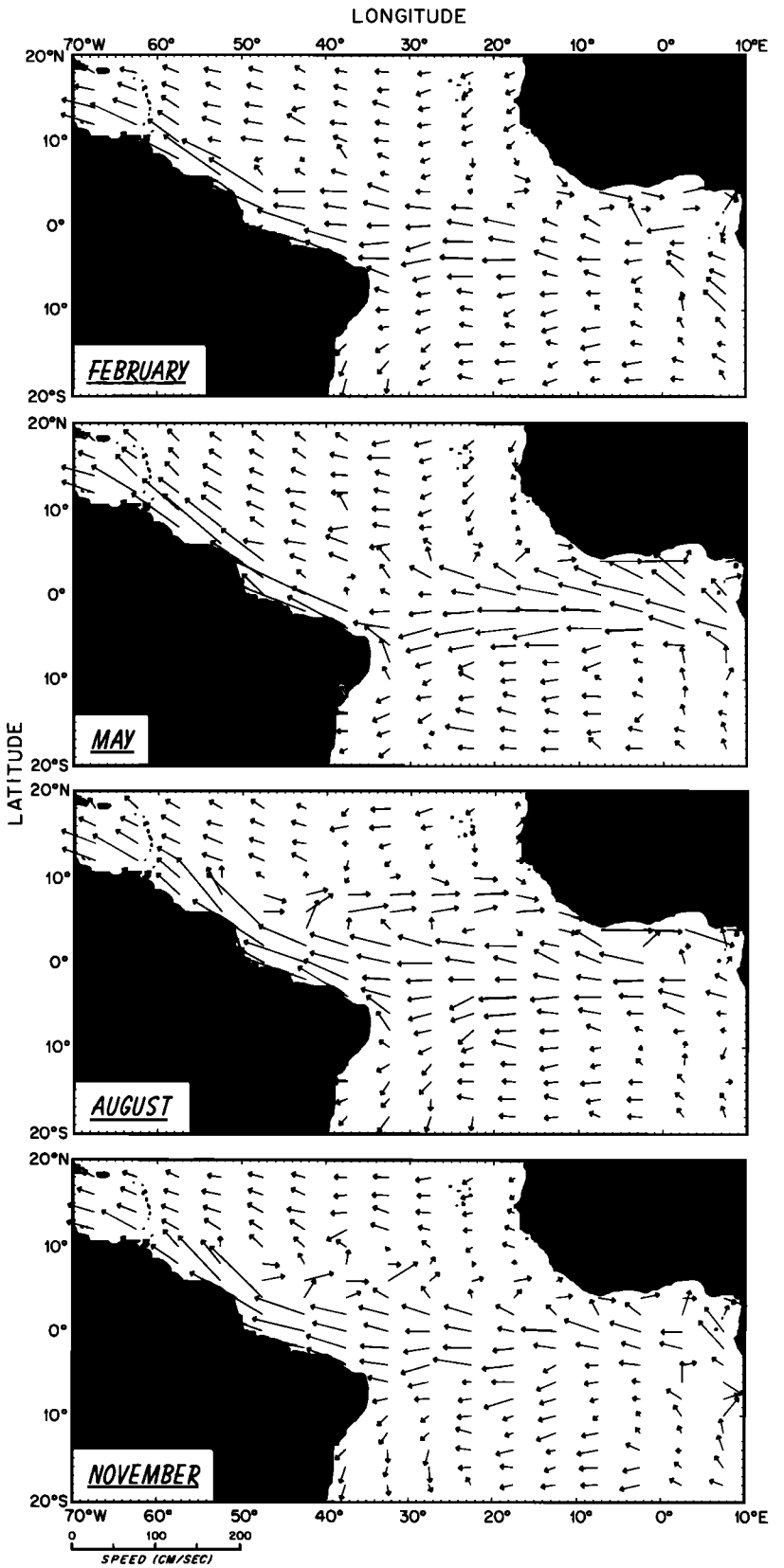

Fig. 4. Maps of velocity vectors for February, May, August, and November, which illustrate the variation of currents throughout the year. Speed is proportional to the length of the tail of a vector.

zonal band of high values (~70%) is evident in the SEC along 5°S, from 5° to 20°W. In general, low values are found on the equator. Over the whole area studied, about 49% of the seasonal variance is due to the annual harmonic, and 69% of the variance is accounted for by a combination of the annual and semiannual harmonics.

Two large regions of nearly constant phase angles occur: one in the NECC and the other in the SEC (Figure 8). In the

TABLE 1. Characteristic Velocity and Seasonal Variation of Tropical Currents

Current	Characteristic Values of Velocity, cm/s			
	Mean Speed	Seasonal Variation	Annual Harmonic	Semiannual Harmonic
Caribbean Current	35	5	4	3
Guyana Current	40	10	10	3
North Brazil Current	75	16	14	6
Brazil Current	10	5	5	1
Guinea Current	40	15	12	6
North Equatorial Current	14	4	3	2
North Equatorial Countercurrent	5–10	20	15	5
South Equatorial Current (SEC)	14	5	2	2
SEC, 2°N	30	15	10	10
SEC, 4°S	30	10	6	5

Characteristic velocity values for the individual currents were chosen subjectively from the maps, which often showed large geographical variations. The reader should consult specific maps for details of the velocity distributions.

NECC, phases become progressively later from east (~230°) to west (~290°), implying a westward phase speed of roughly 60 cm/s. This trend continues eastward into the Guinea Current (~170°) and westward into the Guyana and Caribbean currents (~300°). The SEC shows nearly constant phases (~330°) in a region centered in the eastern Atlantic (2°N–6°S, 10°E–20°W). A thin band of constant phase (~350°) extends westward from this region along 6°S to the western boundary and into the North Brazil Current.

At about 22°W on the equator there is a large (~150°) phase shift, from about 300° between 8°W and 20°W, to 90° west of 22W. Another large phase shift of almost 180° occurs between the NECC and the western SEC, and between the Guinea Current and the eastern SEC. These phase differences cause large fluctuations in the velocity shear between these currents. Outside of the higher-velocity regions the phase is noisy, and trends are difficult to detect.

6.2. *Semiannual Harmonic*

Small semiannual harmonic amplitudes, <2 cm/s, are seen along the western, northern, and southern boundaries (Figure 6). The amplitudes increase to more than 10 cm/s in a band which lies along 2°N and extends from the eastern boundary in the Gulf of Guinea out to 33°W. Amplitudes are large (>12 cm/s) in the east and gradually decrease westward to about 5 cm/s at the western boundary. Throughout the NECC, amplitudes are small, typically 5 cm/s.

The semiannual harmonic accounts for >30% of the seasonal variance in an equatorial band extending across the Atlantic between 3°S and 3°N (Figure 7). A region in which >50% is accounted for is centered in the mid-Atlantic, between 20°W and 33°W. The highest values are 84% at 0°N, 22.5°W and 58% at 0°N, 7.5°W. Over the entire tropical Atlantic region, 20% of the seasonal variance is due to semiannual oscillations.

A striking pattern seen in Figure 8 is the westward phase propagation in the equatorial band, between 3°N and 5°S. At 7.5°E the phase is ~120°, in the mid-Atlantic it is 180°, and at 32.5°W it is 210°, implying a westward phase speed of roughly 100 cm/s. West of 35°W the pattern becomes more complicated. Since the ocean response to wind forcing contains eastward and westward propagating waves along the equator and reflections off the boundaries, and since data from many years are lumped together, one should be very cautious about attributing a phase propagation value to a particular wave. In the NECC, phases do not vary much zonally in the band between 5°N and 8°N, although they do change markedly from north to south. However, at 10°N a westward phase propagation can be seen, with phase speeds of roughly 75 cm/s. North and south of 4°N there is a 180° shift which could contribute to seasonally varying shear between the NECC and SEC.

6.3. *Discussion of Harmonics*

In summary, the annual harmonic accounts for most of the seasonal variation in the western boundary currents, the NECC, and the Guinea Current. The semiannual harmonic accounts for most of the seasonal variation in the part of the SEC near the equator in the mid-Atlantic. Annual and semiannual harmonics make nearly equal contributions to the seasonal variation of the SEC in the Gulf of Guinea.

The region of large variability in the western NECC corresponds to a region of high seasonal variability in wind stress, which also is dominated by an annual period [*Busalacchi and Picaut*, 1983; *Hellerman*, 1980; *Hastenrath and Lamb*, 1977]. This region coincides latitudinally with the mean position of the intertropical convergence zone, which shifts north and south annually. This meridional shifting of the ITCZ causes annual period variations in the curl of the wind stress which are out of phase on opposite sides of the mean position of the ITCZ. The curl of the wind stress tilts the thermocline meridionally across the axis of the NECC by Ekman pumping and divergence of the geostrophic currents [*Garzoli and Katz*, 1983; *Merle*, 1983; *Busalacchi and Picaut*, 1983]. Maps of the time-longitude distribution of thermocline tilt [*Garzoli and Katz*, 1983] and zonal velocity in the NECC [*Richardson and McKee*, 1984] are very similar. If one assumes that the tilt of thermocline is an indication of near-surface geostrophic velocity, then the implication is that variations in ship drift velocity agree with variations in geostrophic velocity. The local wind drives an Ekman flow which could add to the geostrophic response. However, since the climatological wind does not blow eastward (in the western NECC), the swift eastward current velocity there cannot be an Ekman surface current.

The second region of large variability, located near the equator in the Gulf of Guinea, does not correspond to a region of large variability in wind stress. Wind stress along the equator has a dominant annual period, an amplitude which increases from east to west, and a westward phase

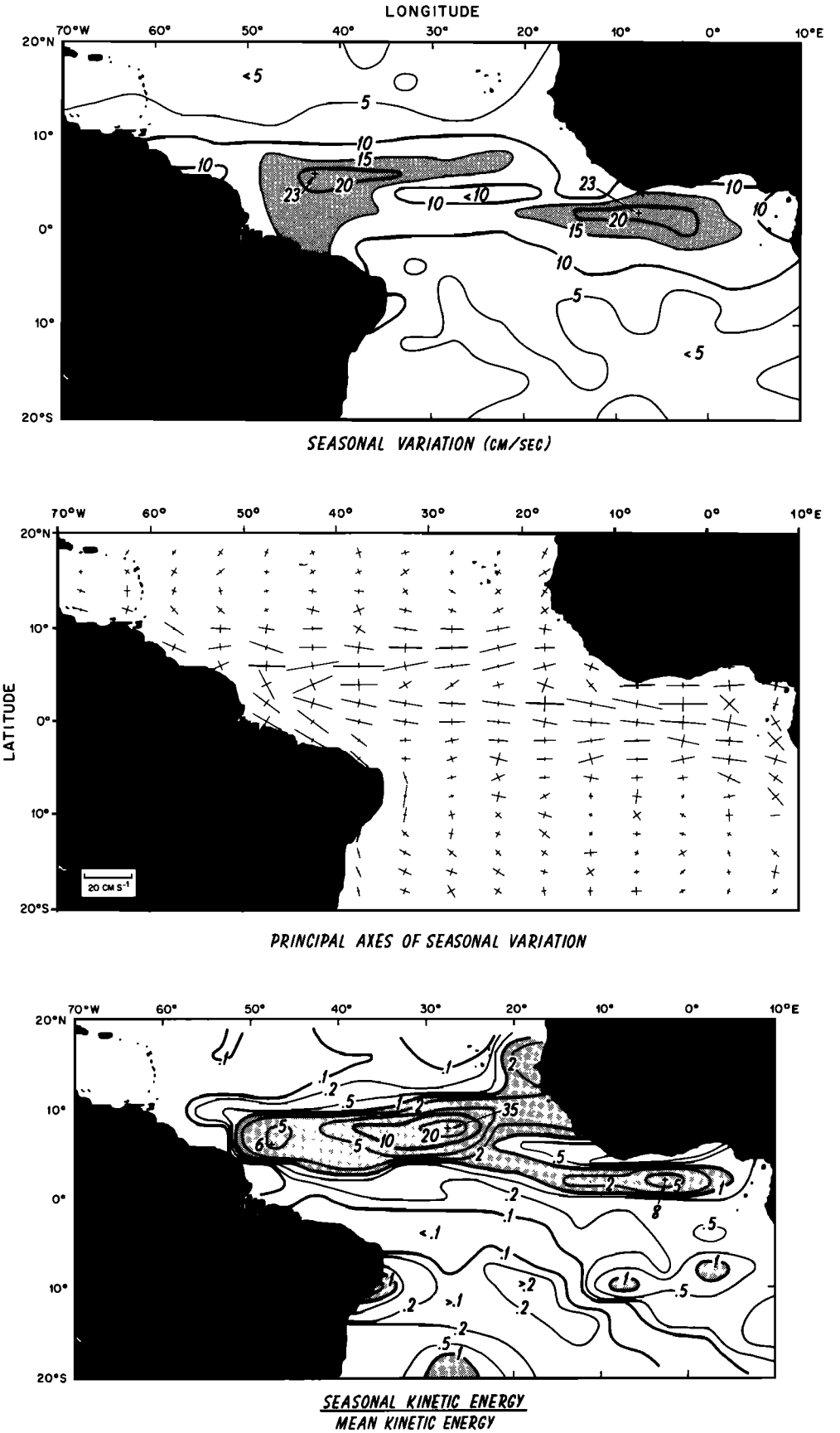

Fig. 5. (Top) Amplitude (in centimeters per second) of the seasonal variation of the 12 average monthly velocity values in each 2° × 5° box, (middle) amplitude and orientation of the principal axes of the seasonal variation of velocity, and (bottom) ratio of the energy of the seasonal variation to the kinetic energy of the annual mean velocity, which we define to be $(\langle u'u' \rangle + \langle v'v' \rangle)/(\langle u \rangle^2 + \langle v \rangle^2)$. Large values in the ratio occur where the seasonal variation is large and/or the mean velocity is small.

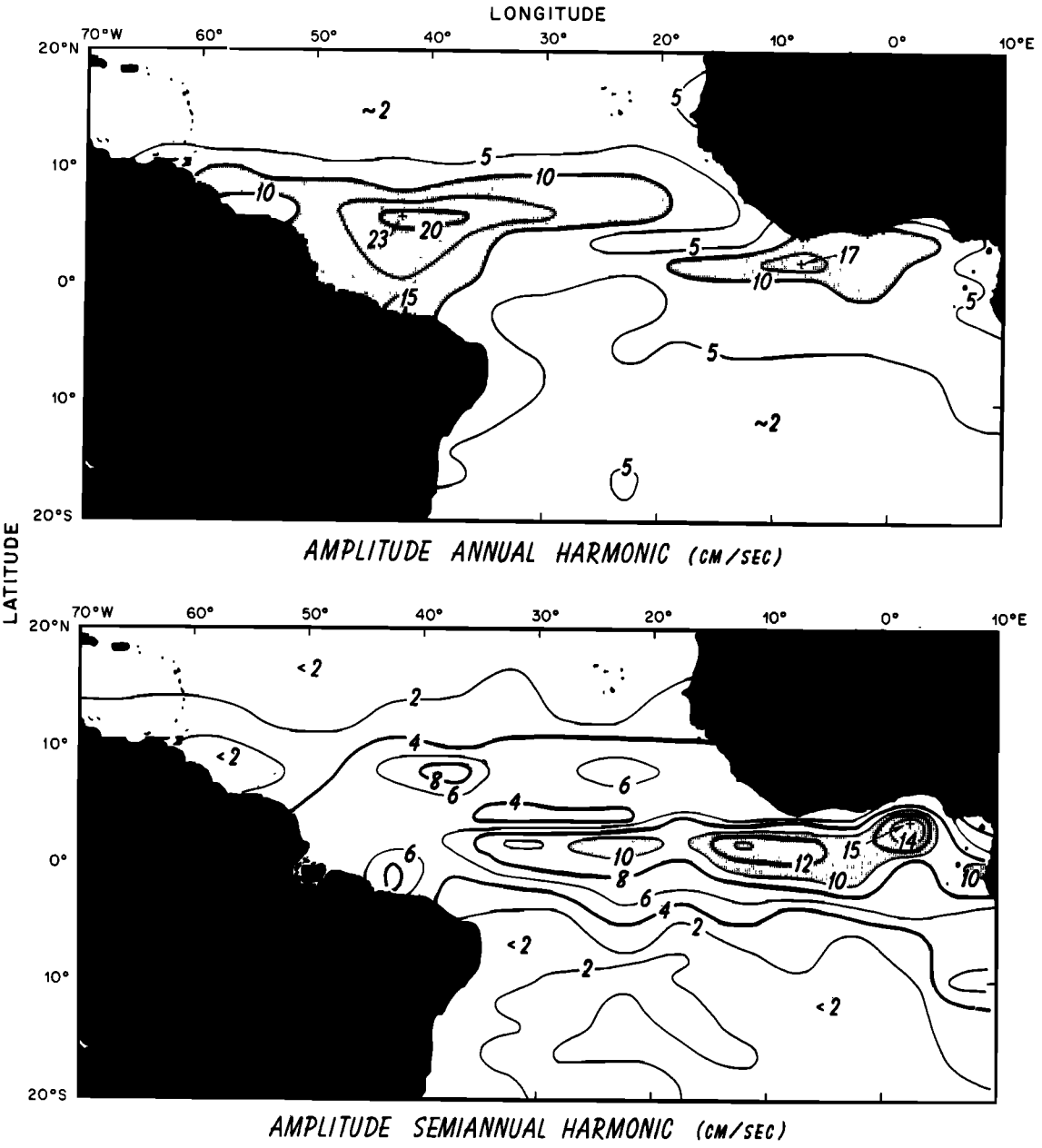

Fig. 6. Amplitude (in centimeters per second) of the annual and semiannual harmonics calculated from the 12 monthly values.

propagation [*Busalacchi and Picaut*, 1983; *Picaut*, 1983]. The large variability of the currents in the Gulf of Guinea appears to be due to a combination of local and remote forcing. The ocean response is complicated near the equator; a thorough understanding will require further analysis of historical and SEQUAL-FOCAL data, as well as numerical simulations. The semiannual fluctuations along the equator have recently been studied by *Philander and Pacanowski* [1986], who find them to be due in part to a natural resonance of the equatorial band and partly to the semiannual wind forcing. The amplitude and timing of these two components combine to give the observed velocity variations. This resonance effect was seen by increasing the modeled wind to its seasonal maximum and then by keeping the wind constant with time. Afterward, the modeled zonal currents slowly decayed with time, while at the same time oscillating with a semiannual period.

7. Empirical Orthogonal Functions

The first two EOFs, accounting for 35% and 29% of the variance, respectively, are shown in Figure 9. Each EOF consists of 197 vectors that are simultaneously modulated by the principal component time series, as was described earlier. These figures help show how fluctuations in one part of the ocean are linked with simultaneous fluctuations in other areas. The EOFs pertain only to the fluctuating, or residual, component of the velocity field. Therefore when an EOF indicates an eastward residual velocity, this will not necessarily be reflected by eastward velocities in the actual

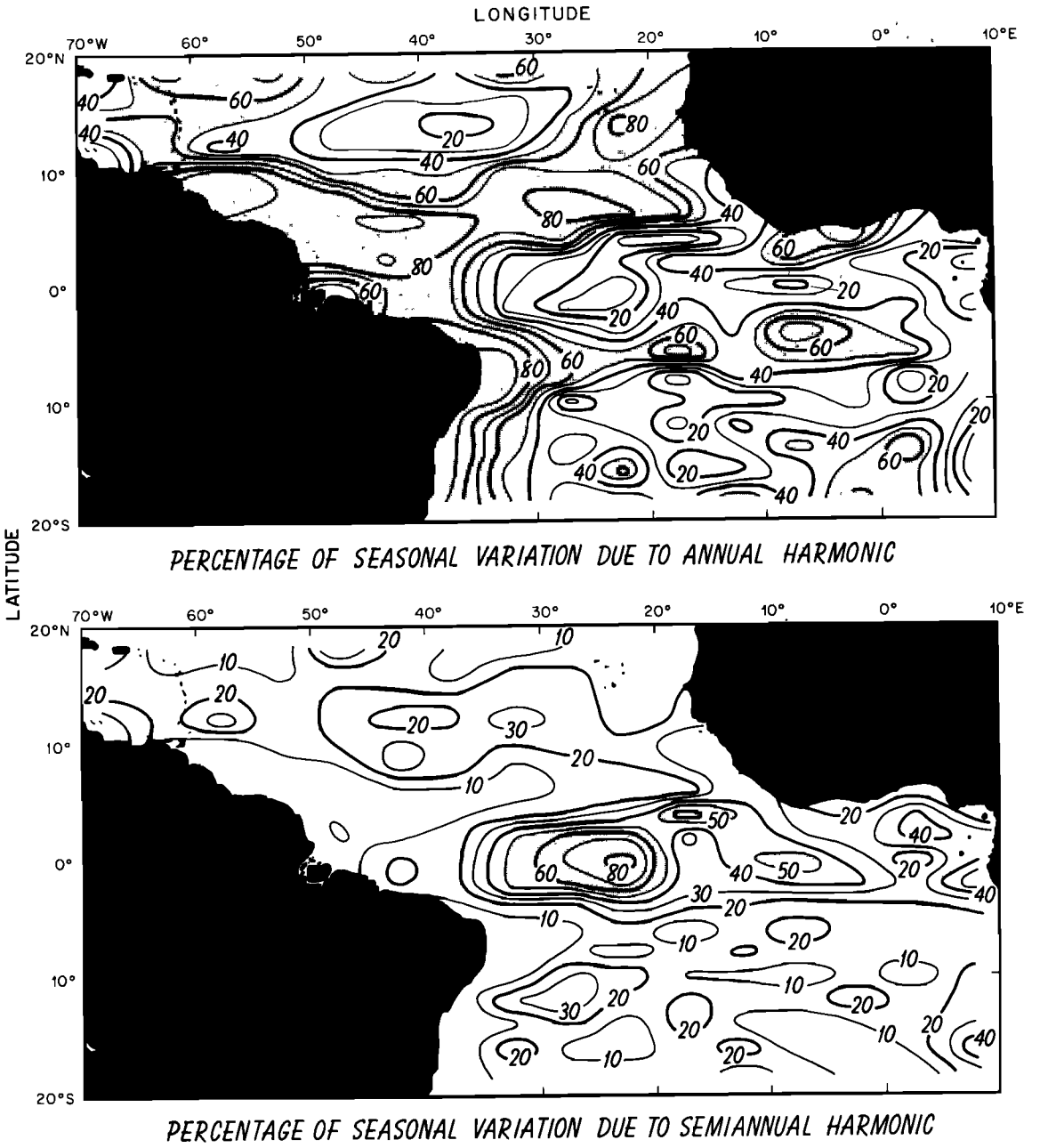

Fig. 7. Percentage of variance of the seasonal variation accounted for by the annual and semiannual harmonics.

velocity field, as annual average velocities must also be taken into account.

7.1. *Second EOF*

The second EOF makes the most sense intuitively; it represents a simultaneous speeding up (slowing down) of the major equatorial currents. The SEC (especially noticeable at 2°N), the North Brazil Current, the NECC, and the Guinea Current all show simultaneous increases (decreases) in velocity. Associated with this pattern is an alongshore residual flow off the coast of South America, from the Brazil Current around the eastern tip of Brazil and into the North Brazil Current. A weak eastward residual flow in the vicinity of the Guyana Current feeds into the NECC. Thus the fluctuations of the major currents coincide with oscillating alongshore flow off South America from 10°N to 20°S. This EOF has two major extrema: the first is between January and April, when the NECC is gone and the SEC is weak, and a second, larger one is evident in July, when the NECC flows rapidly eastward and the SEC is also strong.

7.2. *First EOF*

The overall pattern between 5°S and 10°N for this mode indicates large, in-phase oscillations in the SEC east of 25°W, and in the band between 5°N and 10°N, including the NECC and the Guyana Current. Two large extrema are seen, one in May, and another in September and October. The first corresponds to increased velocities in the SEC and the Guyana Current and decreased velocities in the NECC. The second indicates high velocities in the NECC and low

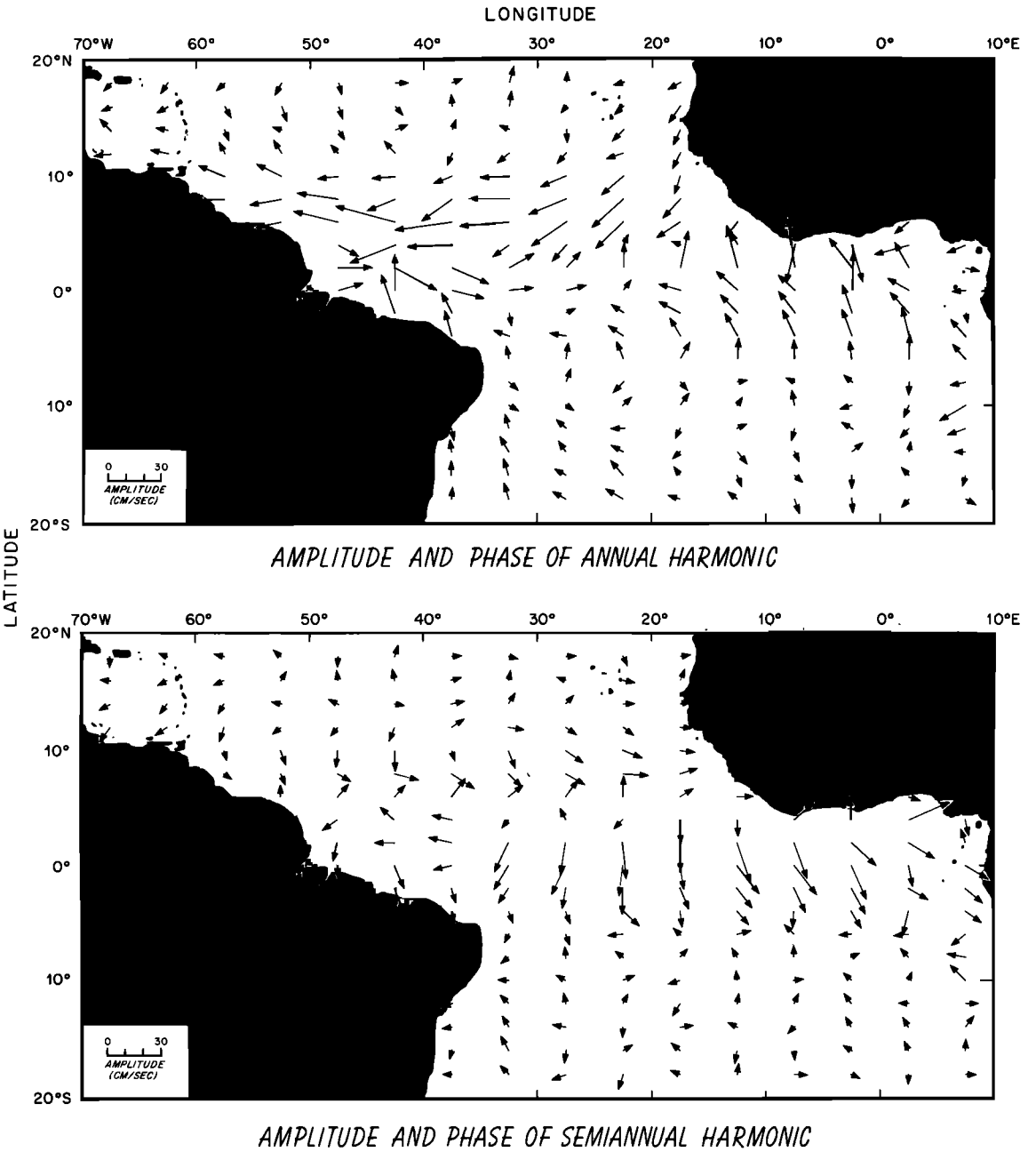

Fig. 8. Amplitude and phase of the annual and semiannual harmonics for the zonal velocity component. The length of the tail of each arrow is proportional to the amplitude of the harmonic. The direction of an arrow gives its phase, with 0° represented by a northward arrow and with phase increasing in a clockwise sense. For the annual harmonic the phase in degrees is nearly equal to the year day of peak eastward residual velocity, while for the semiannual harmonic the phase in degrees is about twice the year day of peak eastward residual velocity.

velocities in the SEC and the Guyana Current. South of 5°N the pattern is more complicated. At about 25°W the vectors show a reversal of the residual velocities in the SEC (north of the equator), with the velocities in the region extending eastward to the African coast in opposition to those in the west. The principal components for this EOF indicate that there will be a convergent tendency in this area in the first part of the year and divergent tendencies later on. Further to the west, in the North Brazil Current, there is an area of strong seasonal convergence/divergence located just east of the Amazon, at about 45°W, 0°–2°N. In this area, strong convergent tendencies are evident early in the year (peaking in May), and divergent tendencies are apparent later on, peaking in September and October. The complex patterns off the coast of South America will be discussed in greater detail in connection with Figure 10.

The third EOF (10% of the variance) consists mainly of meridional velocity vectors in the mid-ocean region, and large-scale patterns are difficult to detect. Because of the apparent noisiness of this EOF, we attribute little physical significance to this mode and therefore do not show it.

The components of the first two EOFs generally point in opposite directions north of 4°N and in the same direction south of it. Combining the two time series for these (sub-

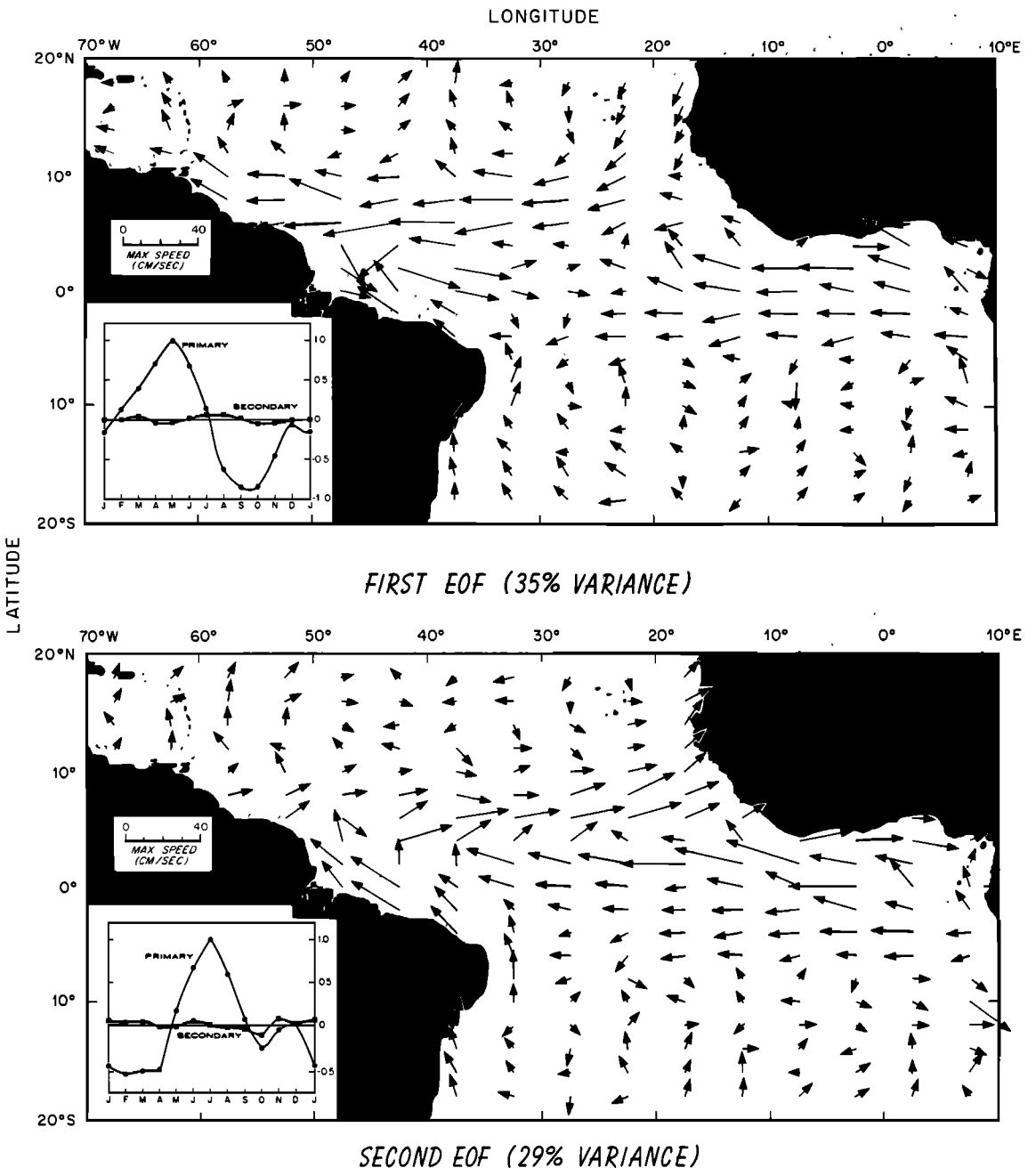

Fig. 9. Velocity vectors and time series expansions for the first two EOFs, which account for 35% and 29%, respectively, of the total variance of the seasonal signal. The vectors are multiplied by the principal component time series given in the inset in the lower left corner. The primary component corresponds to the component of variation parallel to the vectors; the secondary component indicates fluctuations normal to the vectors, causing them to rotate. Since the magnitudes of the primary series are much larger than those of the secondary series, the majority of the variation is parallel to the vectors.

tracting north of 4°N and adding south of 4°N) tends to reproduce the annual period of the variability north of 4°N and the semiannual period south of 4°N.

7.3. *Discussion of EOFs*

To investigate the complicated phenomena off the northeast coast of South America more closely, we divided this region into 1° × 2° boxes and computed EOFs (Figure 10). Only the first EOF is shown, as it is by far the most significant in terms of variance explained. The region of strong seasonal convergence seen near 45°W, 0°–2°N in Figure 9 is clearer in this plot. It appears to be a large discontinuity within the North Brazil Current, indicating that the velocity fluctuations for this mode are out of phase east and west of 45°W. A similar discontinuity is apparent farther up the coast of South America at about 51°W, between the North Brazil Current and the Guyana Current.

The overall pattern for this EOF indicates three coherent bands: (1) the area north of about 3°N, including the Guyana Current and the western NECC; (2) the area immediately south of this, between about 2°S and 2°N, including the westernmost parts of the SEC and the North Brazil Current;

and (3) the part of the North Brazil Current east of 45°W. The northern and southern bands fluctuate together, while the middle band is out of phase with both of these. Fast eastward flow in the NECC is seen to be associated with increased velocities in the northern SEC (2°S–2°N) and decreased velocities in the Guyana Current. These observations seem to indicate that the North Brazil Current east of 45°W and the northern SEC (2°S–2°N) adjust to compensate for one another. When westward velocities in the SEC are high in the second half of the year, westward velocities in the North Brazil Current are low. In the early part of the year, when the NECC has vanished and westward velocities in the SEC are low, velocities in the eastern North Brazil Current are high.

The SEC is out of phase with the North Brazil Current (30°–45°W) because of the annual spring passage of the ITCZ, the eastward flow near the equator, and the start up of the NECC. During April–June the northwestern SEC stops and the North Brazil Current speeds up. This pattern agrees with subsurface measurements. *Metcalf and Stalcup* [1967] used maps of April–June salinity, temperature, and oxygen and concluded that much of the upper 150–200 m of the North Brazil Current (which they call the North Brazil Coastal Current) curves to the right and nearly back on itself in vicinity of the Amazon mouth, forming the eastward flowing Equatorial Undercurrent. They suggest that the undercurrent is fed almost exclusively by South Atlantic water via the North Brazil Current. C. N. Flagg and S. McDowell (unpublished manuscript, 1985) reach a rather similar conclusion. A comparison of the first EOF with their maps of water types shows a close similarity of their eastward flow and the eastward residual flow of the first EOF near 0°N, 40°W in April–June. Thus the ship drifts appear to be revealing the surface manifestation of this subsurface flow.

The maximum northwestward velocity in the North Brazil Current (in May) is associated with northward residual velocities all along the east coast of Brazil. This is seen in both EOFs (Figure 9), which show coherent variations in the flow from 18°S up to the Amazon. Thus the startup of the NECC in May appears to be linked to residual northward flow along the South American coast. Alongshore velocities in the Brazil Current vary by about 10 cm/s within the year, about the same magnitude as the annual mean velocity in this current. Since Brazil Current and North Brazil Current water originates in the SEC, we conclude that the part of the SEC that impinges on the eastern tip of Brazil exhibits strong seasonal fluctuations, much like a switch that is set southward toward the Brazil Current for half a year then reset northward toward the North Brazil Current for the other half year. The amount of water that moves northward and crosses the equator seems to be dependent on this switch. One can imagine shifts in the timing of the switch causing large year-to-year variations in meridional flow.

The linkage between the North Brazil Current, the Guyana Current, and the NECC was investigated by grouping individual velocity observations into larger boxes that spanned each of the currents. The North Brazil Current box includes the western SEC in order to circumvent the problem of the complicated structure off the Amazon as discussed above. The results reveal that the variations in the alongshore velocity of the North Brazil Current and the Guyana Current are nearly 180° out of phase. The North

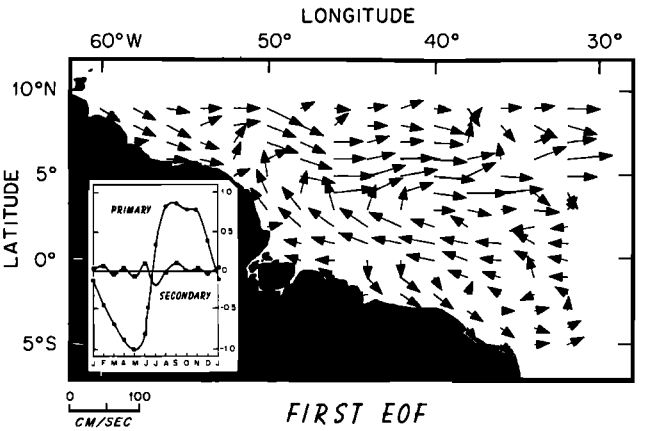

Fig. 10. First EOF (36% of the variance) using a finer grid, 1° × 2°, in order to resolve the flow patterns in vicinity of the Amazon. The time modulation is almost a pure annual harmonic, with a maximum velocity in the direction of vectors occurring in September and a maximum velocity in the opposite direction in May.

Brazil Current is fastest during the last half of the year, when the Guyana Current is slowest and the NECC flows eastward. Furthermore, the velocity time series of the difference between the alongshore velocities in the North Brazil Current and the Guyana Current is very similar to the time variation of the eastward flow in the NECC. Hence the startup of the NECC is associated with increased velocities in the North Brazil Current and decreased velocities in the Guyana Current. Conversely, when the NECC disappears during the first half of the year, more water from the North Brazil Current continues up the coast and into the Guyana Current, which therefore increases in velocity. Thus the North Brazil–Guyana–NECC current system switches flow on a seasonal basis from northwestward during the first half of the year to eastward during the last half. The amount of water moving northward depends on the timing of this seasonal switch.

8. Summary and Conclusions

Historical ship drifts, when suitably combined and averaged, are a valuable measure of near-surface velocity. These data were used to create maps of the seasonal variation of surface currents in the tropical Atlantic. The main result is a statistical description of the climatology of the forced seasonal response of the tropical Atlantic. Several large-scale patterns of variability were identified, showing the amplitude, period, and timing of the dominant variations. A summary of these is given in the abstract. We think that the maps will be useful in (1) interpreting SEQUAL and FOCAL time series data obtained at a few locations in the equatorial Atlantic and (2) verifying model simulations that use climatological winds to generate currents. A study of the similarities and differences of the patterns obtained here with those in model simulations could lead to a better understanding of the dynamics responsible for the observed currents and their seasonal variations.

Acknowledgments. Funds were provided by National Science Foundation grants OCE82-08744 and OCE82-17112. Terry McKee helped program, calculate, and map; Ruth Davis drafted the final figures, and Mary Ann Lucas typed the manuscript. Sophie Wacongne, Susan Schwartz, and Theresa McKee made valuable

suggestions on an earlier version of this paper. Woods Hole Oceanographic Institution contribution 6069.

REFERENCES

Arnault, S., Variation saisonnière de la topographie dynamique et de la circulation superficielle de l'océan Atlantique tropical, thèse de 3e cycle, 198 pp., Universite Pierre et Marie Curie et Museum National d'Histoire Naturelle, Paris, 1984.

Boisvert, W. E., Major currents in the North and South Atlantic Oceans between 64°N and 60°S, *Tech. Rep. TR-193*, 105 pp., Nav. Oceanogr. Office, Suitland, Md., 1967. (Available as NTIS AD-827-58619, Natl. Tech. Inf. Serv., Springfield, Va.)

Busalacchi, A. J., and J. Picaut, Seasonable variability from a model of the tropical Atlantic Ocean, *J. Phys. Oceanogr.*, *13*, 1564–1588, 1983.

Cane, M. A., and E. S. Sarachik, Equatorial oceanography (U.S. National Report to International Union of Geodesy and Geophysics, 1979–1980), *Rev. Geophys.*, *21*, 1137–1148, 1983.

Duncan, C. P., and S. G. Schladow, World surface currents from ship's drift observations, *Int. Hydrogr. Rev.*, *58*, 101–112, 1981.

Fuglister, F. C., Annual variations in current speeds in the Gulf Stream system, *J. Mar. Res.*, *10*, 119–127, 1951.

Garzoli, S. L., and E. J. Katz, The forced annual reversal of the Atlantic North Equatorial Countercurrent, *J. Phys. Oceanogr.*, *13*, 2082–2090, 1983.

Hardy, D. M., and J. J. Walton, Principal components analysis of vector wind measurements, *J. Appl. Meteorol.*, *17*, 1153–1162, 1978.

Hastenrath, S., and P. J. Lamb, *Climatic Atlas of the Tropical Atlantic and Eastern Pacific Oceans*, 112 pp., University of Wisconsin Press, Madison, 1977.

Hellerman, S., Charts of the variability of the wind stress over the tropical Atlantic, *Deep-Sea Res.*, *26*, GATE suppl. II, 63–75, 1980.

Katz, E. J., R. L. Molinari, D. E. Cartwright, P. Hisard, H. U. Lass and A. deMesquita, The seasonal transport of the equatorial undercurrent in the western Atlantic (during the Global Weather Experiment), *Oceanol. Acta*, *4*, 445–450, 1981.

Knox, R. A., and D. L. T. Anderson, Recent advances in the study of low-latitude ocean circulation, *Prog. Oceanogr.*, *14*, 259–317, 1985.

Kundu, P. K., and J. S. Allan, Some three dimensional characteristics of low-frequency current fluctuations near the Oregon coast, *J. Phys. Oceanogr.*, *6*, 181–199, 1976.

Legler, D. M., Empirical orthogonal function analysis of wind vectors over the tropical Pacific region. *Bull. Am. Meteorol. Soc.*, *64*, 234–241, 1983.

McNally, G. J., Satellite-tracked drift buoy observations of the near-surface flow in the eastern mid-latitude North Pacific, *J. Geophys. Res.*, *86*, 8022–8030, 1981.

McNally, G. J., and W. B. White, Wind driven flow in the mixed layer observed by drifting buoys during autumn-winter in the mid-latitude North Pacific, *J. Phys. Oceanogr.*, *15*, 684–694, 1985.

Meehl, G. A., Characteristics of surface current flow inferred from a global ocean current data set, *J. Phys. Oceanogr.*, *12*, 538–555, 1982.

Merle, J., Seasonal variability of subsurface thermal structure in the tropical Atlantic Ocean in *Hydrodynamics of the Equatorial Ocean*, edited by J. C. J. Nihoul, pp. 31–49, Elsevier, New York, 1983.

Metcalf, W. G., and M. C. Stalcup, Origin of the Atlantic Equatorial Undercurrent, *J. Geophys. Res.*, *72*, 4959–4975, 1967.

Philander, S. G. H., Variability of the tropical oceans, *Dyn. Atmos. Oceans*, *3*, 191–208, 1979.

Philander, S. G. H., and R. C. Pacanowski, A model of the seasonal cycle in the tropical Atlantic Ocean. *J. Geophys. Res.*, in press, 1986.

Picaut, J., Propagation of the seasonal upwelling in the eastern equatorial Atlantic. *J. Phys. Oceanogr.*, *13*, 18–37, 1983.

Richardson, P. L., Eddy kinetic energy in the North Atlantic from surface drifters, *J. Geophys. Res.*, *88*, 4355–4367, 1983.

Richardson, P. L., Average velocity and transport of the Gulf Stream near 55°W, *J. Mar. Res.*, *43*, 83–111, 1985.

Richardson, P. L., and T. K. McKee, Average seasonal variation of the Atlantic equatorial currents from historical ship drifts, *J. Phys. Oceanogr.*, *14*(7), 1226–1238, 1984.

Schumacher, A., Monatskarten des oberflachenstromungen im Nordatlantischen Ozean, *Ann. Hydrogr. Mar. Meteorol.*, *68*, 109–123, 1940.

Schumacher, A., Monatskarten des oberflachenstromungen im equatorialen und sudlichen Atlantischen ozean, *Ann. Hydrogr. Mar. Meterol.*, *71*, 209–219, 1943.

SEQUAL, SEQUAL: A study of the equatorial Atlantic Ocean, *Eos Trans. AGU*, *63*, 218, 1982.

Stidd, C. K., Meridional profiles of ship drift components, *J. Geophys. Res.*, *80*, 1679–1682, 1975.

U.S. Naval Oceanographic Office, *Atlas of Pilot Charts, Central American Waters and South Atlantic Ocean, Publ. 106*, 16 pp., Defense Mapping Agency Hydrographic Center, Washington, D.C., 1955.

U.S. Naval Oceanographic Office, Pilot charts of the North Atlantic Ocean, 16 Ser., 12 charts, Defense Mapping Agency Hydrographic Center, Washington, D.C., 1979.

Weisberg, R. H., SEQUAL/FOCAL: First year results on the circulation in the equatorial Atlantic, *Geophys. Res. Lett.*, *11*, 713–714, 1984.

Wyrtki, K., L. Magaard, and J. Hager, Eddy energy in the ocean, *J. Geophys. Res.*, *81*, 2641–2646, 1976.

P. L. Richardson and D. Walsh, Woods Hole Oceanographic Institution, Woods Hole, MA 02543.

(Received December 24, 1985;
accepted February 10, 1986.)